Soluble TREM2 induces inflammatory responses and enhances microglial survival

Li Zhong,[1]* Xiao-Fen Chen,[1,2]* Tingting Wang,[1] Zhe Wang,[1] Chunyan Liao,[1] Zongqi Wang,[1] Ruizhi Huang,[1] Daxin Wang,[1] Xinxiu Li,[1] Linbei Wu,[1] Lin Jia,[1] Honghua Zheng,[1] Meghan Painter,[3] Yuka Atagi,[3] Chia-Chen Liu,[3] Yun-Wu Zhang,[1] John D. Fryer,[3,4] Huaxi Xu,[1,5] and Guojun Bu[1,3,4]

[1]Fujian Provincial Key Laboratory of Neurodegenerative Disease and Aging Research, Institute of Neuroscience, Medical College, Xiamen University, Xiamen 361102, China
[2]Shenzhen Research Institute of Xiamen University, Shenzhen 518063, China
[3]Department of Neuroscience and [4]Neurobiology of Disease Graduate Program, Mayo Clinic, Jacksonville, FL 32224
[5]Neuroscience and Aging Research Center, Sanford-Burnham-Prebys Medical Discovery Institute, La Jolla, CA 92037

Triggering receptor expressed on myeloid cells 2 (TREM2) is an innate immune receptor expressed in microglia in the brain. A soluble form of TREM2 (sTREM2) derived from proteolytic cleavage of the cell surface receptor is increased in the preclinical stages of AD and positively correlates with the amounts of total and phosphorylated tau in the cerebrospinal fluid. However, the physiological and pathological functions of sTREM2 remain unknown. Here, we show that sTREM2 promotes microglial survival in a PI3K/Akt-dependent manner and stimulates the production of inflammatory cytokines depending on NF-κB. Variants of sTREM2 carrying AD risk-associated mutations were less potent in both suppressing apoptosis and triggering inflammatory responses. Importantly, sTREM2 delivered to the hippocampi of both wild-type and *Trem2*-knockout mice elevated the expression of inflammatory cytokines and induced morphological changes of microglia. Collectively, these data indicate that sTREM2 triggers microglial activation inducing inflammatory responses and promoting survival. This study has implications for the pathogenesis of AD and provides insights into targeting sTREM2 pathway for AD therapy.

INTRODUCTION

TREM2 is a member of the Ig superfamily that contains an ectodomain, a transmembrane domain, and a short cytoplasmic tail (Bouchon et al., 2000). In the central nervous system, TREM2 is mainly expressed in microglia and regulates the production of inflammatory cytokines, phagocytosis of apoptotic neuron, and cell survival (Painter et al., 2015). Mutations in the *TREM2* gene have been reported in a spectrum of neurodegenerative disorders, including Nasu-Hakola disease (also known as polycystic lipomembranous osteodysplasia with sclerosing leukoencephalopathy; Paloneva et al., 2002; Klünemann et al., 2005; Numasawa et al., 2011), frontotemporal dementia (Guerreiro et al., 2013b; Borroni et al., 2014; Le Ber et al., 2014), and Alzheimer's disease (AD; Guerreiro et al., 2013a; Jonsson et al., 2013; Jin et al., 2014; Korvatska et al., 2015). Mutations in TREM2 occur primarily within the ectodomain and have been reported to impair ligand binding or protein maturation (Kleinberger et al., 2014; Atagi et al., 2015; Wang et al., 2015).

The arginine 47 to histidine (R47H) substitution in the extracellular immunoglobulin domain significantly increases the risk for AD with an odds ratio similar to that of carrying an apolipoprotein E (*APOE*) ε4 allele (Guerreiro and Hardy, 2013; Guerreiro et al., 2013a; Jonsson et al., 2013). How the R47H mutation modulates disease risk remains to be elucidated; however, existing evidences suggest that it impairs the binding ability of TREM2 to ligands, including phospholipids and apoE (Atagi et al., 2015; Bailey et al., 2015; Wang et al., 2015). The R62H mutation has also been identified to significantly increase the risk of AD (Jin et al., 2014, 2015), whereas the T66M andY38C mutations of TREM2 have been linked to frontotemporal dementia–like syndrome without bone pathology (Guerreiro et al., 2013b). Interestingly, these mutations impair the transport and processing of TREM2, as well as TREM2-regulated phagocytic function (Kleinberger et al., 2014).

One intriguing feature of the TREM2 protein is that it undergoes proteolytic cleavage by ADAM proteases, releasing its ectodomain into the extracellular space as a soluble form (sTREM2; Wunderlich et al., 2013; Kleinberger et al., 2014). Importantly, sTREM2 is abundantly detected in human plasma and cerebrospinal fluid (CSF); and its CSF levels are elevated in AD, multiple sclerosis and other neurological inflammatory diseases (Piccio et al., 2008, 2016; Heslegrave et al., 2016). More interestingly, the amounts of sTREM2 peak

*L. Zhong and X.-F. Chen contributed equally to this paper.

Correspondence to Guojun Bu: bu.guojun@mayo.edu; or Xiao-Fen Chen: chenxf@xmu.edu.cn

Abbreviations used: AD, Alzheimer's disease; CSF, cerebrospinal fluid; sTREM2, soluble TREM2; TREM2, triggering receptor expressed on myeloid cells 2.

The Rockefeller University Press $30.00
J. Exp. Med. 2017 Vol. 214 No. 3 597–607
https://doi.org/10.1084/jem.20160844

The Journal of Experimental Medicine

in the early symptomatic phase of AD and are positively associated with the amounts of total and phosphorylated tau in the CSF (Piccio et al., 2016; Suárez-Calvet et al., 2016). These observations may reflect correlated changes of soluble TREM2 production, microglial activation, and AD-related pathologies. Despite these intriguing findings, it remains unclear what biological or pathological roles sTREM2 plays and how its pathogenic mutations impact these functions. In this study, we examined the effects of sTREM2 on microglial functions using primary cultures and relevant mouse models, and further analyzed the effects of AD-related mutations. We found that sTREM2 has dual roles in promoting the production of inflammatory cytokines and in stimulating microglial survival.

RESULTS AND DISCUSSION

sTREM2 enhances microglial cell viability

To define the roles of sTREM2 in microglia, we first assayed the impact of sTREM2 on microglial cell viability. The extracellular domain of TREM2 spanning the N-terminal aa 1–171 was fused with human IgG-Fc and purified from conditioned media of transfected HEK293T cells (Fig. 1 A). This TREM2-Fc fusion protein was used to mimic the soluble form of TREM2, with Fc alone serving as a negative control. Silver staining of purified proteins under denaturing and reducing conditions in polyacrylamide gels confirmed that the proteins were purified to near homogeneity (Fig. 1 B). Granulocyte macrophage colony-stimulating factor (GM-CSF) is a known stimulator that promotes the proliferation and cell viability of microglia in primary cultures (Lee et al., 1994; Tomozawa et al., 1996). Interestingly, we found that the presence of sTREM2-Fc fusion protein, but not Fc alone, significantly enhanced the cell viability of primary microglia isolated from WT mice, with an effect similar to GM-CSF (Fig. 1 C). Intriguingly, sTREM2-Fc fusion protein also increased the cell viability of primary microglia isolated from *Trem2*-KO mice, indicating that the effect was independent of endogenous, full-length TREM2 (Fig. 1 C). Additionally, the protective effect of sTREM2 on microglial survival was specific for active sTREM2, as the activity was lost upon heat inactivation (Fig. 1 D). In contrast, sTREM2 had no effect on cell proliferation of primary microglia isolated from either wild-type or *Trem2*-KO mice (Fig. 1 E). To further dissect the mechanism by which sTREM2 enhances microglial cell viability, we analyzed the effect of sTREM2 on apoptosis induced by GM-CSF withdrawal. We found that sTREM2 administration resulted in attenuation of apoptosis resulting from GM-CSF withdrawal in primary microglia from WT mice, as well as *Trem2*-KO mice (Fig. 1 F). This protective function was again dependent on active sTREM2, as heat inactivation attenuated the effect. As expected, apoptosis upon GM-CSF withdrawal was markedly increased in primary microglia from *Trem2*-KO mice compared with WT mice (Wang et al., 2015). Interestingly, this effect was fully rescued by sTREM2 administration (Fig. 1 F). Together, these results indicate that sTREM2 exhibits a protective effect on microglial cell viability through a mechanism that is independent of the endogenous, full-length TREM2. Previous studies have shown that full-length TREM2 provides a signal that is necessary for the survival of microglia at low CSF-1 concentrations (Wang et al., 2015). How TREM2 maintains microglial survival remains to be solved. Based on our data, full-length TREM2 might exert its role in promoting cell survival through its proteolytic product sTREM2. The increased level of apoptosis in *Trem2*-KO primary microglia might be attributed to the fact that those cells are unable to generate sTREM2. In our study, a concentration of soluble TREM2 at 20 nM was used to assess the effects on microglial activity in primary cultured cells. Several recent studies have reported that the levels of soluble TREM2 in the CSF of MCI-AD and AD dementia patients were in the 3–6 ng/ml range (~0.17–0.33 nM; Gispert et al., 2016; Piccio et al., 2016; Suárez-Calvet et al., 2016). However, the concentration of soluble TREM2 in the brain, in particular the interstitial fluid remains unknown. Thus, the physiological and pathophysiological relevance of our studies will need to be addressed in future studies under physiologically relevant conditions, including genetic mouse models and perhaps soluble TREM2 isolated from human brains or CSF.

sTREM2 triggers inflammatory responses in microglia

Given that the CSF levels of sTREM2 are elevated in neuroinflammatory diseases including AD and multiple sclerosis (Piccio et al., 2008, 2016; Heslegrave et al., 2016), we next investigated whether sTREM2 affects the inflammatory responses in microglia. We treated primary cultures of microglia with increasing doses of sTREM2 and measured the mRNA levels of IL-1β, IL-6, TNF, IL-10, Arginase 1 (Arg-1), and Ym-1 by quantitative real-time PCR. sTREM2-Fc, but not Fc alone, significantly increased the mRNA levels of inflammatory cytokines IL-1β, IL-6, TNF, and IL-10 in a dose-dependent manner (Fig. 2 A). However, sTREM2 treatment has minimal effects on the expression of Arg-1 and Ym-1, which are M2-specific markers. Therefore, it is unlikely that sTREM2 affects the transcriptional programs globally in microglia. Given that TREM2 is an innate immunoreceptor that inhibits neuroinflammation (Zhong et al., 2015), we hypothesized that sTREM2 may act as a decoy receptor that competes with the full-length TREM2 for the binding of ligand, thereby triggering inflammatory responses in microglia. However, the expression levels of proinflammatory cytokines (IL-1β, IL-6, and TNF) in *Trem2*-KO primary microglia were also significantly increased by sTREM2 treatment (Fig. 2 B). These results indicate that the activation of proinflammatory responses by sTREM2 in microglia occurs through a mechanism that is independent of the endogenous, full-length TREM2. Interestingly, sTREM2 triggered an activated morphology of microglial cells with ovaloid cytoplasm and marked cellular hypertrophy (Fig. 2 C). Quantitatively, the values for several parameters, including area, diame-

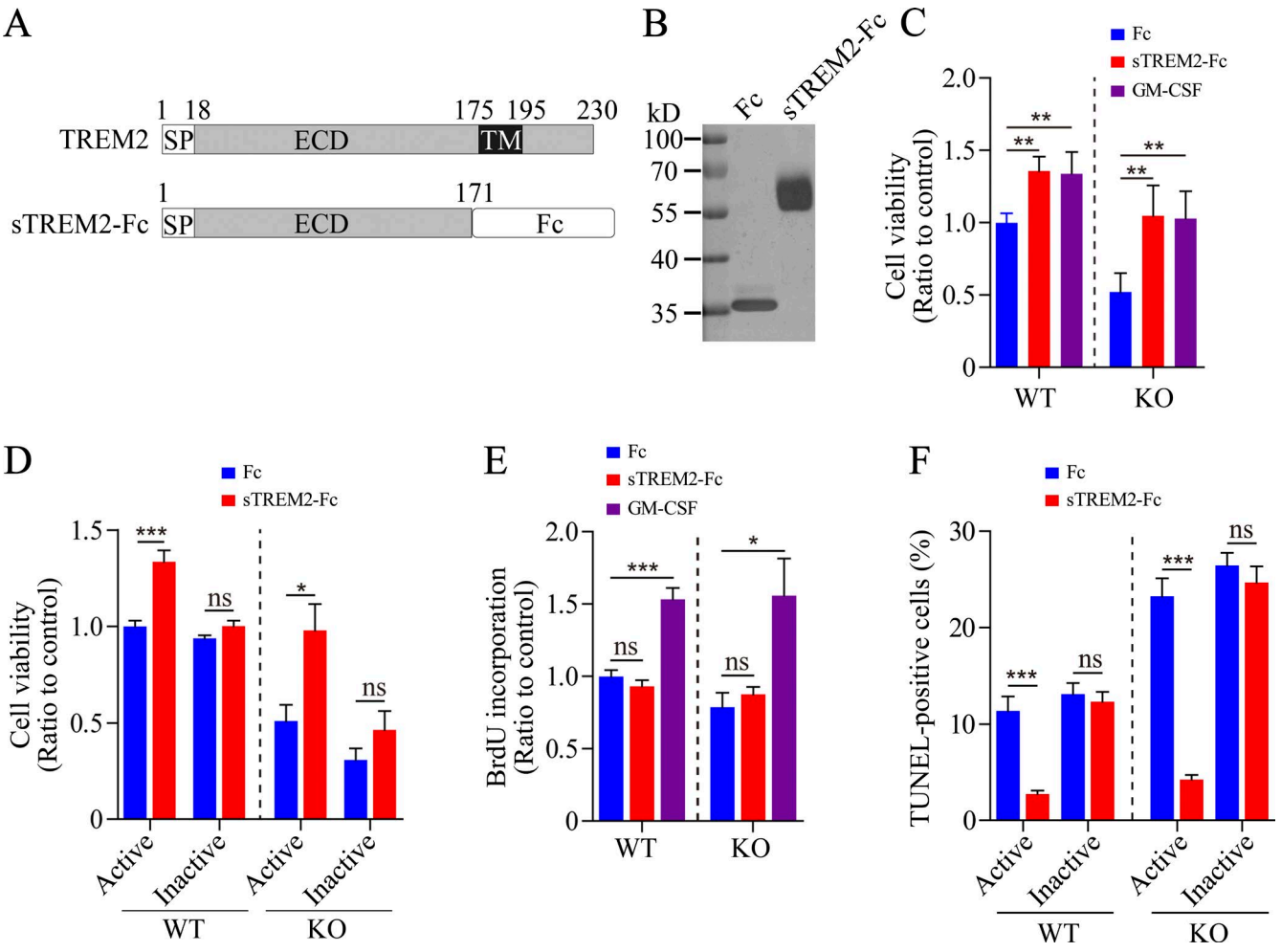

Figure 1. **sTREM2 promotes cellular viability and suppresses cellular apoptosis in microglia.** (A) Schematic representation of full-length human TREM2 and sTREM2-Fc fusion proteins. SP, signal peptide; ECD, extracellular domain; TM, transmembrane domain. (B) The purified Fc and sTREM2-Fc fusion proteins were analyzed by silver staining. (C) The cell viability of WT and *Trem2*-KO microglia were analyzed after cultured with Fc (20 nM), sTREM2-Fc fusion protein (20 nM), or GM-CSF (25 ng/ml) for 24 h ($n = 4$ per group, one-way ANOVA). The cell viability of Fc-treated WT microglia served as a control. (D) The cell viability of WT and *Trem2*-KO microglia were analyzed after culture with 20 nM active (native) or inactive (heat-inactivated for 1.5 h) Fc or sTREM2-Fc protein for 24 h after GM-CSF withdrawal (at least three repeats per group, unpaired Student's *t* test). The cell viability of active Fc-treated WT microglia served as a control. (E) The proliferation of WT and *Trem2*-KO microglia were analyzed after cultured with Fc (20 nM), sTREM2-Fc protein (20 nM) or GM-CSF (25 ng/ml) for 24 h ($n = 4$ per group, one-way ANOVA). The BrdU incorporation rate of Fc-treated WT microglia served as a control. (F) Microglia from WT or *Trem2*-KO mice were cultured with 20 nM active (native) or inactive (heat-inactivated for 1.5 h) Fc or sTREM2-Fc protein for 24 h after GM-CSF withdrawal. TUNEL staining was then performed and 12 different fields from three independent experiments were selected to quantify the number of TUNEL-positive cells (unpaired Student's *t* test). Data represent mean ± SEM. *, $P < 0.05$; **, $P < 0.01$; ***, $P < 0.001$; ns, not significant.

ter, and perimeter, were significantly increased by the presence of sTREM2 (Fig. 2 D).

We have also generated an untagged version of sTREM2 that can be purified to near homogeneity after TEV cleavage (Fig. S1, A and B). We found that this untagged sTREM2 also promoted the survival of primary microglia and increased the expression of proinflammatory cytokines similar to the Fc-tagged sTREM2 (Fig. S1, C and D). To ensure that the functions of sTREM2 are not specific to the human form, we constructed the mouse form of soluble Trem2 with Fc tag (sTrem2-Fc) and purified the protein to near homogeneity (Fig. S1, E and F). Consistently, this mouse form of sTrem2 significantly inhibited microglial apoptosis and increased the expression of inflammatory cytokines (Fig. S1, G and H). Therefore, the effects of sTREM2 on microglial survival and inflammatory responses are conserved between mouse and human in our experimental systems. In addition, we found that the function of sTREM2 in microglia was independent of DAP12, the adaptor protein that initiates TREM2 intracellular signaling (Fig. S2, A–C).

Collectively, these results support a role of sTREM2 in the activation of microglia. Because TREM2 signaling

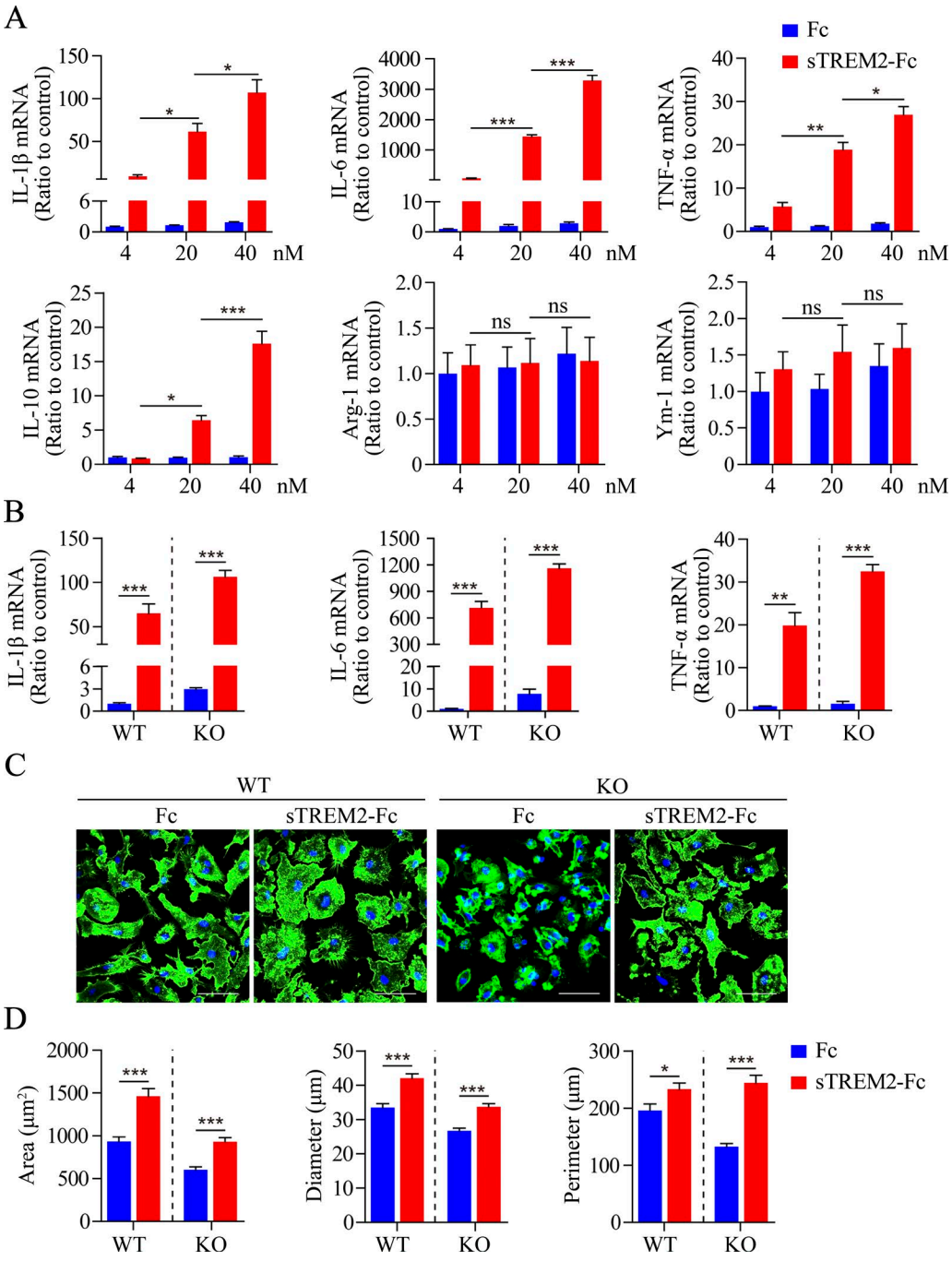

Figure 2. **sTREM2 promotes the production of inflammatory cytokines.** (A) Primary microglia were treated with 4, 20, or 40 nM purified Fc or sTREM2-Fc fusion protein for 4 h. RNA was extracted, and the relative mRNA levels of IL-1β, IL-6, TNF, IL-10, Arg-1, and Ym-1 shown as bar graph were determined by quantitative real-time PCR. β-Actin was used as an internal control (n = 3 per group, one-way ANOVA). The mRNA level of 4 nM Fc-treated microglia served as a control. (B) Primary microglia isolated from WT or *Trem2*-KO were treated with 20 nM purified Fc or sTREM2-Fc fusion protein for 4 h. RNA was extracted and the relative mRNA levels of IL-1β, IL-6, and TNF shown as bar graphs were determined by quantitative real-time PCR. β-Actin was used as an internal control (n = 3 per group, unpaired Student's t test). The mRNA level of Fc-treated WT microglia served as a control. (C) WT or *Trem2*-KO microglia were treated with 20 nM Fc or sTREM2-Fc fusion proteins for 24 h. Microglia were then stained by Alexa Fluor 488–labeled phalloidin. Representative photomicrographs are shown (blue, DAPI; green, phalloidin). Bar, 50 µm. (D) At least 55 cells from three independent experiments were selected to quantify the size of microglia, including area, diameter, and perimeter (unpaired Student's t test). Data represent mean ± SEM. *, $P < 0.05$; **, $P < 0.01$; ***, $P < 0.001$.

has been portrayed as antiinflammatory in myeloid cells including microglia, our present results provide a paradigm in which sTREM2 acts independently of, and perhaps plays an opposing role against the full-length TREM2 in regulating inflammatory responses.

sTREM2 activates the Akt–GSK3β–β-catenin and the NF-κB signaling pathways in microglia

Emerging evidence suggests that the Akt–GSK3β–β-catenin pathway plays a critical role in cellular apoptosis (Song et al., 2005; Zhu et al., 2014). Consistently, the higher proportion of apoptotic cells associated with *Trem2*-KO microglia was correlated with reductions of signaling components of the Akt–GSK3β–β-catenin pathway (Fig. 3, A and B). The levels of phospho-Akt (Ser473), phospho-GSK3β (Ser9), and β-catenin were significantly reduced in *Trem2*-KO microglia, as compared with WT control. We further investigated whether sTREM2 exerts its antiapoptotic effect by modulating the Akt–GSK3β–β-catenin pathway. As shown in Fig. 3 A, sTREM2 treatment increased the phosphorylation of Akt on serine 473 and the phosphorylation of GSK3β on serine 9. Furthermore, sTREM2 treatment markedly increased the levels of β-catenin in microglia isolated from both WT and *Trem2*-KO mice. Interestingly, the activation of Akt–GSK3β–β-catenin pathway by sTREM2 was attenuated by the presence of a PI3K/Akt inhibitor, LY-294002 (Fig. 3, C and D). Remarkably, drug treatment reversed the levels of β-catenin, the phosphorylation of Akt on serine 473, and the phosphorylation of GSK3β on serine 9 that were increased by sTREM2 back to the levels in Fc-nontreated group. Under this condition, sTREM2 could no longer rescue microglial cells from apoptosis upon GM-CSF withdrawal (Fig. 3 E). It was suggested that sTREM2 triggers the activation of ERK1/2 kinase to promote macrophage survival (Wu et al., 2015). However, in our studies, sTREM2 suppressed apoptosis by activating the Akt–GSK3β–β-catenin survival pathway in microglia.

To identify the signaling pathway that mediates sTREM2-induced proinflammatory responses, we pretreated primary microglia with various compounds that specifically block individual signaling pathways, including the transcription factor NF-κB and each of the major MAP kinase subtypes (ERK1/2, JNK, and p38). The mRNA levels of proinflammatory cytokines (IL-1β, IL-6, and TNF) were not changed in the presence or absence of JNK inhibitor SP600125 (Fig. 3 F). The inhibitors for p38-MAPK (SB203580) and ERK1/2 (U0126) only significantly decreased the expression level of IL-1β, but not IL-6 and TNF. In contrast, the inhibitor for NF-κB, Bay 11–7082, markedly down-regulated the production of all three proinflammatory cytokines (Fig. 3 F). Supporting a role of the NF-κB pathway, sTREM2 increased the phosphorylation of NF-κB p65 at serine 536, which is essential for its transcriptional activity (Fig. 3, G and H). This effect was attenuated by the presence of a NF-κB inhibitor, Bay 11–7082. We next examined whether the internalization of sTREM2 is necessary for its functions in microglia by immobilizing sTREM2 on culture plates (referred to as isTREM2) to prevent its internalization. We found that this form of sTREM2 also significantly increased the mRNA levels of proinflammatory cytokines (Fig. S3, A–C), indicating that sTREM2 may bind to cell surface receptors to initiate its function in microglia without the need for internalization. Collectively, our data suggest a crucial regulatory role of sTREM2 in activating the Akt–GSK3β–β-catenin and NF-κB signaling pathways, which may account for the antiapoptotic and proinflammatory functions of sTREM2 in microglia. Additional work is needed to define the precise molecular pathways downstream of sTREM2 actions.

The AD risk-associated TREM2 mutations impair the functions of sTREM2

Based on our observation that sTREM2 plays important roles in regulating microglial viability and inflammatory responses, we next investigated whether AD risk-associated variants of TREM2 impair the functions of sTREM2. Arginine residue at aa 47 or 62 substituted with histidine (R47H or R62H) is strongly associated with AD (Guerreiro et al., 2013a; Jonsson et al., 2013; Jin et al., 2014, 2015). We generated cDNA constructs and purified sTREM2-Fc fusion proteins carrying the R47H or R62H mutation from conditioned media of transfected HEK293T cells (Fig. 4 A). The ability of sTREM2 in supporting the antiapoptotic function was markedly reduced by the R47H or R62H mutation compared with that of the WT sTREM2, as measured by TUNEL staining (Fig. 4 B). In addition, the two AD risk-associated variants partially lost their ability to increase the expression levels of proinflammatory cytokines (Fig. 4 C). Together, these data suggest that the AD risk-associated R47H and R62H mutations reduce the overall capacity of sTREM2 to enhance cell viability and to trigger inflammatory responses in microglia. Our results may thus constitute previously unknown molecular mechanisms linking TREM2 variants with increased risk of AD.

sTREM2 triggers inflammatory responses and leads to microglial activation in vivo

To gain a view of the functions of sTREM2 in vivo, we injected sTREM2-Fc protein into the hippocampi of both wild-type and *Trem2*-knockout mice, with Fc alone serving as a control (Fig. 5 A). The injection of sTREM2 significantly increased the expression of inflammatory cytokines IL-1β, IL-6, and TNF in both wild-type and *Trem2*-knockout mice (Fig. 5 B), results that are consistent with the effects on microglia in culture. Microglia in the healthy mature CNS typically show a ramified morphology, including a small soma with fine cellular processes. Upon sTREM2 injection, microglia in both wild-type and *Trem2*-knockout mice showed morphological changes consistent with microglial activation, including significantly decreased cell processes and increased cell body size across the CA3, CA2, and CA1 regions (Fig. 5, C–I). Collectively, these data indicate that sTREM2 triggers

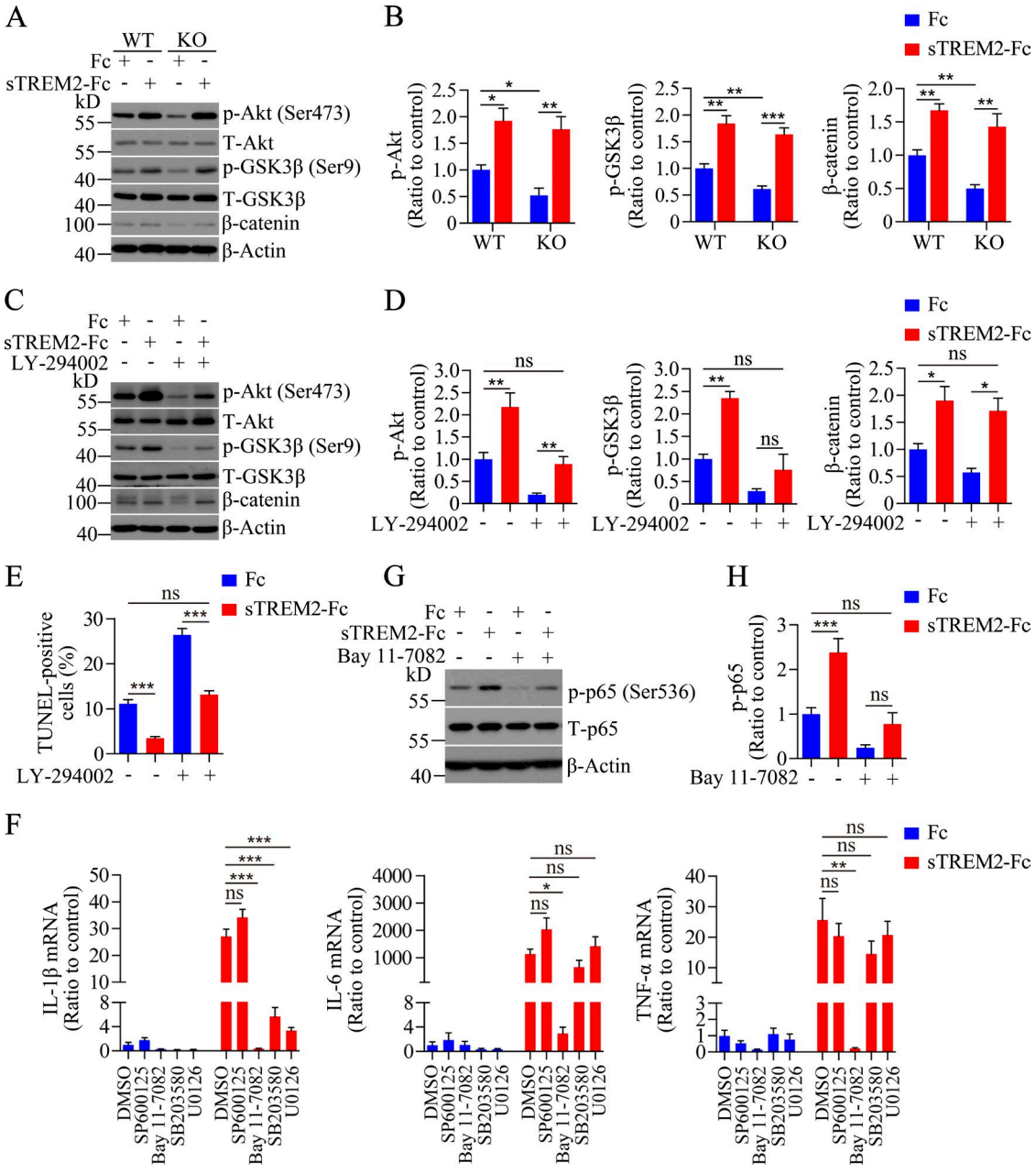

Figure 3. **sTREM2 activates the Akt–GSK3β–β-catenin and the NF-κB signaling pathways in microglia.** (A) Microglia obtained from WT or *Trem2*-KO mice were treated with 20 nM Fc or sTREM2-Fc protein for 24 h after GM-CSF withdrawal. The protein levels of phospho-Akt (p-Akt, Ser473), total-Akt (T-Akt), phospho-GSK3β (p-GSK3β, Ser9), total-GSK3β (T-GSK3β), and β-catenin were analyzed by Western blotting. (B) Quantification of the relative levels of p-Akt, p-GSK3β and β-catenin ($n = 4$ per group, unpaired Student's t test). The protein level of Fc-treated WT microglia served as a control. (C) Microglia from WT mice were pretreated with 25 µM of a PI3K/Akt inhibitor (LY-294002) for 30 min, followed by treatment with 20 nM Fc or sTREM2-Fc protein for 24 h. The protein levels of p-Akt, T-Akt, p-GSK3β, T-GSK3β, and β-catenin were analyzed by Western blotting. (D) Quantification of the relative levels of p-Akt, p-GSK3β, and β-catenin ($n = 3$ per group, one-way ANOVA). The protein level of Fc-treated microglia served as a control. (E) Microglia from WT mice were pretreated with 25 µM of a PI3K/Akt inhibitor (LY-294002) for 30 min, followed by treatment with 20 nM Fc or sTREM2-Fc protein for 24 h. TUNEL assay was then performed and 12 different fields from three independent experiments were selected for quantifying the number of TUNEL-positive cells (one-way ANOVA). (F) Microglia from WT mice were pretreated with 10 µM SP600125, Bay 11–7082, SB203580, or U0126 for 30 min, followed by treatment with 20 nM Fc or sTREM2-Fc protein for 4 h. Real-time PCR analysis was then performed to detect the expression of IL-1β, IL-6, and TNF ($n = 5$ per group, one-way ANOVA). The mRNA level of DMSO- and Fc-treated microglia served as a control. (G) WT microglia were pretreated with 10 µM of a NF-κB inhibitor (Bay 11–7082) for 30 min, followed by treatment with 20 nM Fc or sTREM2-Fc protein for 1 h. The protein levels of phospho-NF-κB p65 (p-p65, Ser536) and

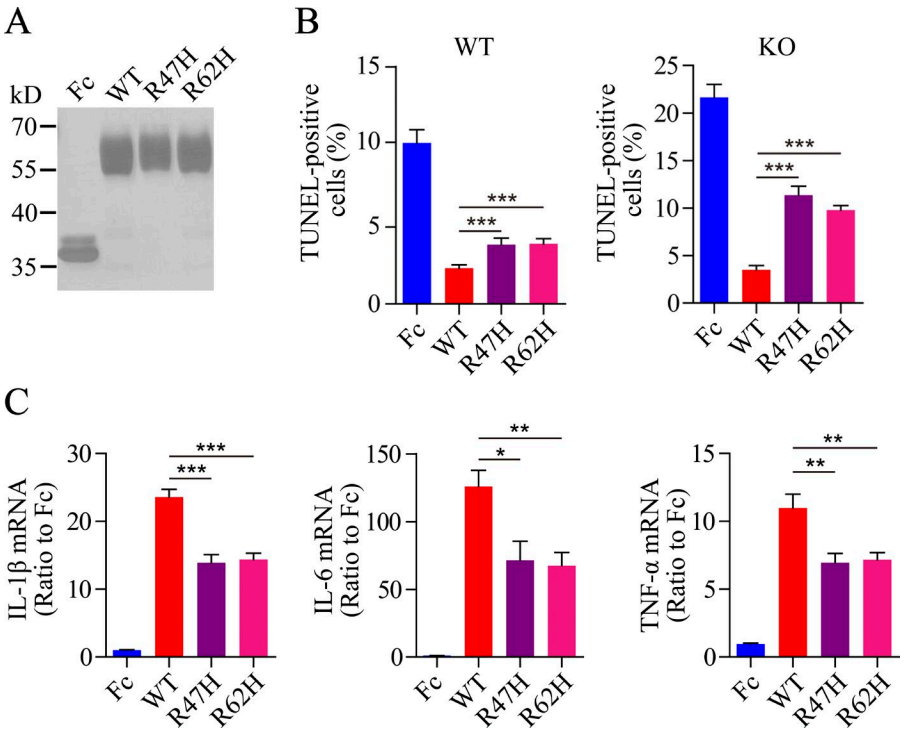

Figure 4. **The AD risk-associated variants impair the functions of sTREM2 in microglia.** (A) The purified Fc, sTREM2 WT-Fc (WT), sTREM2 R47H-Fc (R47H), and sTREM2 R62H-Fc (R62H) fusion proteins were analyzed by silver staining. (B) Microglia obtained from WT or *Trem2*-KO mice were cultured with 20 nM Fc, WT, R47H, or R62H protein for 24 h after GM-CSF withdrawal. TUNEL staining was then performed and 12 different fields from three independent experiments were selected to quantify the number of TUNEL-positive cells (one-way ANOVA). (C) Primary microglia from WT mice were treated with 20 nM Fc, WT, R47H, or R62H protein for 4 h. RNA was extracted and the relative mRNA levels of IL-1β, IL-6, and TNF shown as bar graph were determined by quantitative real-time PCR. β-Actin was used as an internal control (n = 5 per group, one-way ANOVA). Data represent mean ± SEM. *, P < 0.05; **, P < 0.01; ***, P < 0.001.

inflammatory responses and leads to microglial activation both in vitro and in vivo.

In conclusion, our results demonstrate that sTREM2 plays a crucial role in regulating microglial cell survival and inflammatory responses. To our knowledge, this is the first report revealing the biological effects of sTREM2 in microglia. In the context of AD, our most intriguing finding is that the AD risk-associated sTREM2-R47H and sTREM2-R62H variants are less potent in both suppressing apoptosis and triggering proinflammatory responses. Remarkably, our results demonstrate that sTREM2 triggers inflammatory responses and leads to microglial activation in the mouse brain. Collectively, our data suggest that impaired functions of sTREM2 caused by AD-associated mutations may contribute to impaired microglial function in AD and more importantly an exciting possibility that increasing sTREM2 signaling might be an efficacious therapeutic approach to treat AD.

MATERIALS AND METHODS

Reagents and antibodies

p38-MAPK inhibitor (SB203580), ERK1/2 inhibitor (U0126), JNK inhibitor (SP600125), NF-κB inhibitor (Bay 11–7082), Akt inhibitor (LY-294002), and DAPI were purchased from Sigma-Aldrich. GM-CSF was purchased from R&D Systems. Kits for Cell Proliferation Assay (MTS), Dead-End Fluorometric TUNEL System, and TEV protease were purchased from Promega. In Situ Cell Death Detection kit and cOmplete His-Tag Purification Resin were purchased from Roche. BrdU ELISA kit was purchased from Abcam. Protein A Agarose and Alexa Fluor 488 Phalloidin were purchased from Thermo Fisher Scientific. Antibodies for Western blotting used in this study, including anti–Phospho-NF-κB p65 (Ser536), anti–total-NF-κB p65, anti–Phospho-Akt (Ser473), anti–total-Akt, anti-Phospho-GSK3β (Ser9), anti–total-GSK3β, anti–β-catenin, and anti–β-actin, were purchased from Cell Signaling Technology; anti–human TREM2 antibody for Western blotting was purchased from R&D Systems (AF1828). Antibodies for immunofluorescence including anti-Iba1 and anti–human TREM2 were purchased from Wako and Santa Cruz Biotechnology (sc-373828), respectively.

Isolation and culture of mouse primary microglia

Primary microglial cultures were prepared as previously described (Zhu et al., 2010; Atagi et al., 2015). All animal experiments were conducted in compliance with the protocols of the Institutional Animal Care and Use Committee at Xiamen University. In brief, wild-type or *Trem2*-KO mice (C57BL/6N; 3–4 pups) at postnatal day 1–2 were used to prepare mixed glial cultures. Cells were plated onto poly-L-lysine–coated flasks and grown in DMEM supplemented

total-NF-κB p65 (T-p65) were analyzed by Western blotting. (H) Quantification of the relative levels of phospho-NF-κB p65 (p-p65, Ser536; n = 6 per group, one-way ANOVA). The protein level of Fc-treated microglia served as a control. Data represent mean ± SEM. *, P < 0.05; **, P < 0.01; ***, P < 0.001; ns, not significant.

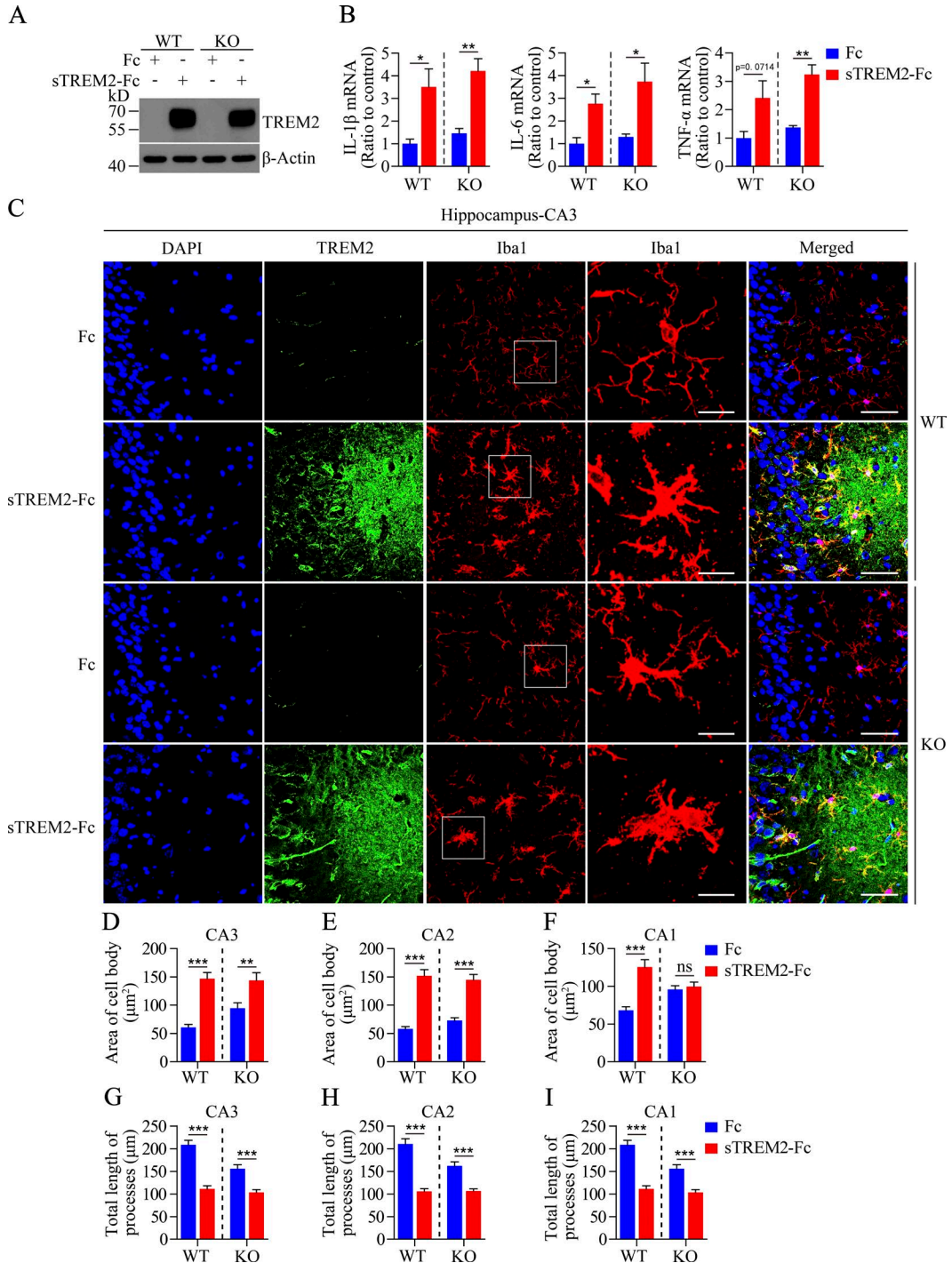

Figure 5. **sTREM2 protein increases the expression of proinflammatory cytokines and induces morphological changes of microglia in mouse brain.** (A) Fc and sTREM2-Fc proteins were analyzed by Western blotting after injection into the hippocampi of WT or *Trem2*-KO mice. (B) The hippocampi were dissected from Fc- or sTREM2-Fc–injected WT or *Trem2*-KO mice. After RNA extraction, the relative mRNA levels of IL-1β, IL-6, and TNF in the hippocampi shown as bar graph were determined by quantitative real-time PCR. β-Actin was used as an internal control ($n = 4$ per group, unpaired Student's t test). The mRNA level of Fc-injected WT mice served as a control. (C) Coronal sections from Fc- or sTREM2-Fc–injected WT or *Trem2*-KO mice were stained with DAPI (blue) for nuclei, TREM2 (green) for sTREM2-Fc protein, and Iba1 (red) for microglia. Representative z stack images of CA3 region are shown. Bar, 50 µm. Iba1-labeled images on the right represent enlarged microglia; bar, 10 µm. (D–I) Analyses of morphological parameters include the area of cell body and total length of processes (D and G for CA3 region, E and H for CA2 region, F and I for CA1 region). At least 30 cells each from three mice were selected to quantify the morphological parameters (unpaired Student's t test). Data represent mean ± SEM. *, $P < 0.05$; **, $P < 0.01$; ***, $P < 0.001$.

with 10% FBS (Gibco). After 3 d, medium was changed so that it contained 25 ng/ml GM-CSF and 10% FBS. Primary microglial cells were harvested by shaking (200 rpm, 20 min) after 10–12 d in culture and once every 3 d thereafter (up to four harvests).

Expression and purification of sTREM2 protein

The human TREM2 extracellular domain (aa residues 1–171) and its variants (R47H and R62H) tagged with Fc were cloned and purified from the culture media of HEK293T cells, as previously described (Atagi et al., 2015). To produce sTREM2 protein without a tag, a TEV-cleavage site was added between sTREM2 and Fc sequence. The sTREM2-TEV-Fc fusion protein was initially purified from the conditioned media by incubating with Protein A agarose and subjected to TEV cleavage. The TEV Protease, which contains an N-terminal His-tag, was subsequently removed by Ni-NTA column after cleavage reaction. The eluted proteins were dialyzed against 1× PBS and filtered through a 0.22-μm filter before use. For heat inactivation, purified Fc or sTREM2-Fc fusion protein was boiled at 100°C for 1.5 h.

RNA isolation and real-time PCR analysis

Total RNA was extracted from primary microglia or hippocampus using TRIzol reagent (Invitrogen). 1 μg RNA was reverse transcribed into first-strand cDNA using ReverTra Ace qPCR RT Master Mix (TOYOBO) according to the manufacturer's protocol. Quantitative PCR was performed using the FastStart Universal SYBR Green Master mix (Roche). The primer sequences used for Il-1β, Il-6, and β-actin were the same as previously described (Zhong et al., 2015). The primer sequences for TNF, Il-10, Arg-1, and Ym-1 were as follows: TNF, forward, 5′-GTCTACTGAACTTCGGGGTGAT-3′, reverse 5′-CTGAGTGTGAGGGTCTGGGC-3′; IL-10, forward, 5′-GCTCTTACTGACTGGCATGAG-3′, reverse, 5′-CGCAGCTCTAGGAGCATGTG-3′; Arg-1, forward, 5′-CACAGTCTGGCAGTTGGAAGC-3′, reverse, 5′-CTTTGGCAGATATGCAGGGAG-3′; Ym-1, forward, 5′-CAGGTCTGGCAATTCTTCTGAA-3′, reverse, 5′-GTCTTGCTCATGTGTGTAAGTGA-3′. All primer sets were purchased from Life Technologies.

Western blotting

Cells were harvested with nonidet-P40 (NP40) lysis buffer (1% NP-40, 50 mM Tris-HCl, pH 8.0, 150 mM sodium chloride supplemented with protease, and phosphatase inhibitors cocktail) and protein concentrations were determined using the BCA protein assay kit according to the manufacturer's instruction (Thermo Fisher Scientific). Equal amounts of total proteins were subjected to sodium dodecyl sulfate-PAGE (SDS-PAGE) and transferred to PVDF membrane (Millipore). Proteins were visualized using ECL Western blotting detection reagents (Millipore). Immunoreactive bands were quantified using ImageJ software (National Institutes of Health).

Cell proliferation assay

WT and *Trem2*-KO primary microglial cells were seeded into 96-well culture plates at a density of 6×10^4 cells/well and were cultured for 48 h after GM-CSF withdrawal. After administration with purified Fc or sTREM2-Fc fusion protein for 24 h, the cell proliferation was assessed using BrdU ELI SA kit (Abcam) according to the manufacturer's instruction.

Cell viability assay

WT and *Trem2*-KO primary microglia cells were seeded into 96-well culture plates at a density of 5×10^4 cells/well and were cultured for 48 h after GM-CSF withdrawal. After administration with purified Fc or sTREM2-Fc fusion protein for 24 h, the cells were assessed for viability using Cell Proliferation Assay (MTS) according to the manufacturer's instruction.

TUNEL assay

WT and *Trem2*-KO primary microglial cells were seeded into 24-well culture plates at a density of 1×10^5 cells/well and were cultured for 48 h after GM-CSF withdrawal. The cells were then treated with purified Fc or sTREM2-Fc fusion protein for 24 h. After washing three times with 1× PBS, the cells were fixed for 15 min with 4% paraformaldehyde (PFA), and then permeabilized with 0.2% Triton X-100 for 5 min. Terminal deoxynucleotidyl transferase-mediated dUTP nick end-labeling (TUNEL) assay was performed with the DeadEnd Fluorometric TUNEL System (Promega) or the In Situ Cell Death Detection kit (Roche) according to the manufacturers' protocol. For DAPI staining, cells were further stained for 1 min, and then washed twice with 0.1% PBST for 15 min. Coverslips were mounted on glass slides using anti-fade reagent (Life Technologies) and observed under A1R Plus confocal microscope (Nikon). After photomicrography, apoptotic nuclei were counted and analyzed.

Stereotaxic injection and preparation of brain samples

WT or *Trem2*-KO mice at 7–8 mo of age were anesthetized and placed in a stereotaxic frame, a skin incision was made and holes were drilled at x (±2.0 mm from bregma) and y (–2.2 mm from bregma). A total of 3 μg in 1.5 μl vol of Fc or sTREM2-Fc protein were delivered at 0.20 μl/min at z-depths of 2.0 mm. The syringe was left in place for 10 min after each injection, before being withdrawn slowly. 24 h after injection, mice were anesthetized and perfused with ice-cold PBS. For biochemical analysis, hippocampi from the left brain were dissected out, snap frozen in liquid nitrogen, and stored at –80°C for extraction of protein and RNA. For histological analysis, right brain hemispheres were fixed in 4% PFA overnight at 4°C and transferred to 30% sucrose for 48 h, before being embedded for cryostat sectioning.

Immunohistochemistry and microscopy

12-μm-thick cryosections were washed in 1× PBS for 15 min, and then permeabilized in 5% normal donkey serum and

0.2% Triton X-100 for 1 h, followed by overnight incubation with TREM2 and Iba1 antibodies at 4°C. The cryosections were washed with 1× PBS for 30 min and treated with the Alexa-fluorophore–conjugated secondary antibodies for 1 h at room temperature. Sections were stained with DAPI (5 µg/ml), washed, and mounted with anti-fade reagent (Life Technologies). For confocal microscopy, 15-µm z-stacks (consisting of 31 optical slices of 0.5 µm thickness) were acquired using an A1R Plus confocal microscope and used for analysis of the areas of microglial cell body and the lengths of processes.

Online supplemental material

Fig. S1 shows the functions of untagged sTREM2 and mouse sTrem2 in microglia. Fig. S2 shows that sTREM2 inhibits microglial apoptosis and induces the production of cytokines independent of DAP12. Fig. S3 shows that sTREM2 can carry out its function in microglia without the need for internalization.

ACKNOWLEDGMENTS

Research by the authors was supported by grants from the National Natural Science Foundation of China 81370459, 31400914 (to X.-F. Chen), and U1505227 (to G. Bu), National Institutes of Health grants R01AG035355, RF1AG051504, R01AG027924, R01AG046205, P01NS074969, and P50AG016574 (to G. Bu), a grant from the Cure Alzheimer's Fund (to G. Bu), a grant from the Fundamental Research Funds for the Central Universities (20720150051 to X.-F. Chen), a grant from the Guangdong Natural Science Foundation (2016A030306005 to X.-F. Chen), a grant from the China Postdoctoral Science Foundation (2016M600503 to L. Zhong), and grants from the Tanz Family Funds and Alzheimer's Association (C4C-15-369446 to H. Xu).

The authors declare no competing financial interests.

Author contributions: L. Zhong, X.-F. Chen and G. Bu designed research; L. Zhong, T. Wang, Z. Wang, C. Liao, Z. Wang, R. Wang, D. Wang, X. Li, L. Wu, and L. Jia performed experiments; L. Zhong, X.-F. Chen, and T. Wang analyzed data; L. Zhong and X.-F. Chen wrote the manuscript; H. Zheng, M. Painter, Y. Atagi, C.-C. Liu, Y.-W. Zhang, J.D. Fryer, H. Xu, and G. Bu reviewed the paper. All authors read and approved the final manuscript.

Submitted: 5 June 2016
Revised: 25 October 2016
Accepted: 24 January 2017

REFERENCES

Atagi, Y., C.C. Liu, M.M. Painter, X.F. Chen, C. Verbeeck, H. Zheng, X. Li, R. Rademakers, S.S. Kang, H. Xu, et al. 2015. Apolipoprotein E Is a Ligand for Triggering Receptor Expressed on Myeloid Cells 2 (TREM2). *J. Biol. Chem.* 290:26043–26050. http://dx.doi.org/10.1074/jbc.M115.679043

Bailey, C.C., L.B. DeVaux, and M. Farzan. 2015. The Triggering Receptor Expressed on Myeloid Cells 2 Binds Apolipoprotein E. *J. Biol. Chem.* 290:26033–26042. http://dx.doi.org/10.1074/jbc.M115.677286

Borroni, B., F. Ferrari, D. Galimberti, B. Nacmias, C. Barone, S. Bagnoli, C. Fenoglio, I. Piaceri, S. Archetti, C. Bonvicini, et al. 2014. Heterozygous TREM2 mutations in frontotemporal dementia. *Neurobiol. Aging.* 35:934.e7–934.e10. http://dx.doi.org/10.1016/j.neurobiolaging.2013.09.017

Bouchon, A., J. Dietrich, and M. Colonna. 2000. Cutting edge: inflammatory responses can be triggered by TREM-1, a novel receptor expressed on neutrophils and monocytes. *J. Immunol.* 164:4991–4995. http://dx.doi.org/10.4049/jimmunol.164.10.4991

Gispert, J.D., M. Suárez-Calvet, G.C. Monté, A. Tucholka, C. Falcon, S. Rojas, L. Rami, R. Sánchez-Valle, A. Lladó, G. Kleinberger, et al. 2016. Cerebrospinal fluid sTREM2 levels are associated with gray matter volume increases and reduced diffusivity in early Alzheimer's disease. *Alzheimers Dement.* 12:1259–1272. http://dx.doi.org/10.1016/j.jalz.2016.06.005

Guerreiro, R., and J. Hardy. 2013. TREM2 and neurodegenerative disease. *N. Engl. J. Med.* 369:1569–1570. http://dx.doi.org/10.1056/NEJMc1306509

Guerreiro, R.J., E. Lohmann, J.M. Brás, J.R. Gibbs, J.D. Rohrer, N. Gurunlian, B. Dursun, B. Bilgic, H. Hanagasi, H. Gurvit, et al. 2013b. Using exome sequencing to reveal mutations in TREM2 presenting as a frontotemporal dementia-like syndrome without bone involvement. *JAMA Neurol.* 70:78–84. http://dx.doi.org/10.1001/jamaneurol.2013.579

Guerreiro, R., A. Wojtas, J. Bras, M. Carrasquillo, E. Rogaeva, E. Majounie, C. Cruchaga, C. Sassi, J.S. Kauwe, S. Younkin, et al. Alzheimer Genetic Analysis Group. 2013a. *TREM2* variants in Alzheimer's disease. *N. Engl. J. Med.* 368:117–127. http://dx.doi.org/10.1056/NEJMoa1211851

Heslegrave, A., W. Heywood, R. Paterson, N. Magdalinou, J. Svensson, P. Johansson, A. Öhrfelt, K. Blennow, J. Hardy, J. Schott, et al. 2016. Increased cerebrospinal fluid soluble TREM2 concentration in Alzheimer's disease. *Mol. Neurodegener.* 11:3. http://dx.doi.org/10.1186/s13024-016-0071-x

Jin, S.C., B.A. Benitez, C.M. Karch, B. Cooper, T. Skorupa, D. Carrell, J.B. Norton, S. Hsu, O. Harari, Y. Cai, et al. 2014. Coding variants in TREM2 increase risk for Alzheimer's disease. *Hum. Mol. Genet.* 23:5838–5846. http://dx.doi.org/10.1093/hmg/ddu277

Jin, S.C., M.M. Carrasquillo, B.A. Benitez, T. Skorupa, D. Carrell, D. Patel, S. Lincoln, S. Krishnan, M. Kachadoorian, C. Reitz, et al. 2015. TREM2 is associated with increased risk for Alzheimer's disease in African Americans. *Mol. Neurodegener.* 10:19. http://dx.doi.org/10.1186/s13024-015-0016-9

Jonsson, T., H. Stefansson, S. Steinberg, I. Jonsdottir, P.V. Jonsson, J. Snaedal, S. Bjornsson, J. Huttenlocher, A.I. Levey, J.J. Lah, et al. 2013. Variant of TREM2 associated with the risk of Alzheimer's disease. *N. Engl. J. Med.* 368:107–116. http://dx.doi.org/10.1056/NEJMoa1211103

Kleinberger, G., Y. Yamanishi, M. Suárez-Calvet, E. Czirr, E. Lohmann, E. Cuyvers, H. Struyfs, N. Pettkus, A. Wenninger-Weinzierl, F. Mazaheri, et al. 2014. TREM2 mutations implicated in neurodegeneration impair cell surface transport and phagocytosis. *Sci. Transl. Med.* 6:243ra86. http://dx.doi.org/10.1126/scitranslmed.3009093

Klünemann, H.H., B.H. Ridha, L. Magy, J.R. Wherrett, D.M. Hemelsoet, R.W. Keen, J.L. De Bleecker, M.N. Rossor, J. Marienhagen, H.E. Klein, et al. 2005. The genetic causes of basal ganglia calcification, dementia, and bone cysts: DAP12 and TREM2. *Neurology.* 64:1502–1507. http://dx.doi.org/10.1212/01.WNL.0000160304.00003.CA

Korvatska, O., J.B. Leverenz, S. Jayadev, P. McMillan, I. Kurtz, X. Guo, M. Rumbaugh, M. Matsushita, S. Girirajan, M.O. Dorschner, et al. 2015. R47H variant of TREM2 associated with Alzheimer disease in a large late-onset family: Clinical, genetic, and neuropathological study. *JAMA Neurol.* 72:920–927. http://dx.doi.org/10.1001/jamaneurol.2015.0979

Le Ber, I., A. De Septenville, R. Guerreiro, J. Bras, A. Camuzat, P. Caroppo, S. Lattante, P. Couarch, E. Kabashi, K. Bouya-Ahmed, et al. 2014. Homozygous TREM2 mutation in a family with atypical frontotemporal dementia. *Neurobiol. Aging.* 35:2419.e23–2419.e25. http://dx.doi.org/10.1016/j.neurobiolaging.2014.04.010

Lee, S.C., W. Liu, C.F. Brosnan, and D.W. Dickson. 1994. GM-CSF promotes proliferation of human fetal and adult microglia in primary cultures. *Glia.* 12:309–318. http://dx.doi.org/10.1002/glia.440120407

Numasawa, Y., C. Yamaura, S. Ishihara, S. Shintani, M. Yamazaki, H. Tabunoki, and J.I. Satoh. 2011. Nasu-Hakola disease with a splicing mutation of TREM2 in a Japanese family. *Eur. J. Neurol.* 18:1179–1183. http://dx.doi.org/10.1111/j.1468-1331.2010.03311.x

Painter, M.M., Y. Atagi, C.C. Liu, R. Rademakers, H. Xu, J.D. Fryer, and G. Bu. 2015. TREM2 in CNS homeostasis and neurodegenerative disease. *Mol. Neurodegener.* 10:43. http://dx.doi.org/10.1186/s13024-015-0040-9

Paloneva, J., T. Manninen, G. Christman, K. Hovanes, J. Mandelin, R. Adolfsson, M. Bianchin, T. Bird, R. Miranda, A. Salmaggi, et al. 2002. Mutations in two genes encoding different subunits of a receptor signaling complex result in an identical disease phenotype. *Am. J. Hum. Genet.* 71:656–662. http://dx.doi.org/10.1086/342259

Piccio, L., C. Buonsanti, M. Cella, I. Tassi, R.E. Schmidt, C. Fenoglio, J. Rinker II, R.T. Naismith, P. Panina-Bordignon, N. Passini, et al. 2008. Identification of soluble TREM-2 in the cerebrospinal fluid and its association with multiple sclerosis and CNS inflammation. *Brain.* 131:3081–3091. http://dx.doi.org/10.1093/brain/awn217

Piccio, L., Y. Deming, J.L. Del-Águila, L. Ghezzi, D.M. Holtzman, A.M. Fagan, C. Fenoglio, D. Galimberti, B. Borroni, and C. Cruchaga. 2016. Cerebrospinal fluid soluble TREM2 is higher in Alzheimer disease and associated with mutation status. *Acta Neuropathol.* 131:925–933. http://dx.doi.org/10.1007/s00401-016-1533-5

Song, G., G. Ouyang, and S. Bao. 2005. The activation of Akt/PKB signaling pathway and cell survival. *J. Cell. Mol. Med.* 9:59–71. http://dx.doi.org/10.1111/j.1582-4934.2005.tb00337.x

Suárez-Calvet, M., G. Kleinberger, M.A. Araque Caballero, M. Brendel, A. Rominger, D. Alcolea, J. Fortea, A. Lleó, R. Blesa, J.D. Gispert, et al. 2016. sTREM2 cerebrospinal fluid levels are a potential biomarker for microglia activity in early-stage Alzheimer's disease and associate with neuronal injury markers. *EMBO Mol. Med.* 8:466–476. http://dx.doi.org/10.15252/emmm.201506123

Tomozawa, Y., T. Inoue, M. Takahashi, M. Adachi, and M. Satoh. 1996. Apoptosis of cultured microglia by the deprivation of macrophage colony-stimulating factor. *Neurosci. Res.* 25:7–15. http://dx.doi.org/10.1016/0168-0102(96)01021-8

Wang, Y., M. Cella, K. Mallinson, J.D. Ulrich, K.L. Young, M.L. Robinette, S. Gilfillan, G.M. Krishnan, S. Sudhakar, B.H. Zinselmeyer, et al. 2015. TREM2 lipid sensing sustains the microglial response in an Alzheimer's disease model. *Cell.* 160:1061–1071. http://dx.doi.org/10.1016/j.cell.2015.01.049

Wu, K., D.E. Byers, X. Jin, E. Agapov, J. Alexander-Brett, A.C. Patel, M. Cella, S. Gilfilan, M. Colonna, D.L. Kober, et al. 2015. TREM-2 promotes macrophage survival and lung disease after respiratory viral infection. *J. Exp. Med.* 212:681–697. http://dx.doi.org/10.1084/jem.20141732

Wunderlich, P., K. Glebov, N. Kemmerling, N.T. Tien, H. Neumann, and J. Walter. 2013. Sequential proteolytic processing of the triggering receptor expressed on myeloid cells-2 (TREM2) protein by ectodomain shedding and γ-secretase-dependent intramembranous cleavage. *J. Biol. Chem.* 288:33027–33036. http://dx.doi.org/10.1074/jbc.M113.517540

Zhong, L., X.F. Chen, Z.L. Zhang, Z. Wang, X.Z. Shi, K. Xu, Y.W. Zhang, H. Xu, and G. Bu. 2015. DAP12 Stabilizes the C-terminal Fragment of the Triggering Receptor Expressed on Myeloid Cells-2 (TREM2) and Protects against LPS-induced Pro-inflammatory Response. *J. Biol. Chem.* 290:15866–15877. http://dx.doi.org/10.1074/jbc.M115.645986

Zhu, W., H. Zheng, X. Shao, W. Wang, Q. Yao, and Z. Li. 2010. Excitotoxicity of TNFalpha derived from KA activated microglia on hippocampal neurons in vitro and in vivo. *J. Neurochem.* 114:386–396. http://dx.doi.org/10.1111/j.1471-4159.2010.06763.x

Zhu, X., S. Wang, L. Yu, H. Yang, R. Tan, K. Yin, J. Jin, H. Zhao, D. Guan, and Y. Xu. 2014. TL-2 attenuates β-amyloid induced neuronal apoptosis through the AKT/GSK-3β/β-catenin pathway. *Int. J. Neuropsychopharmacol.* 17:1511–1519. http://dx.doi.org/10.1017/S1461145714000315